Photon-assisted shot noise in the mesoscopic system with a toroidal carbon nanotube coupled to normal-metal leads perturbed by ac fields

Hong-Kang Zhao[1,2] and Jian Wang[1]
[1]*Department of Physics and the Center of Theoretical and Computational Physics, The University of Hong Kong, Pokfulam Road, Hong Kong, China*
[2]*Department of Physics, Beijing Institute of Technology, Beijing 100081, China**
(Received 23 May 2006; revised manuscript received 16 August 2006; published 1 December 2006)

We have investigated the shot noise of a system with a toroidal carbon nanotube (TCN) coupled to two metal leads with applied microwave fields. The tunneling current operator is derived by determining the electron operators in different parts of the system. The Landauer-Büttiker-like current operator is also obtained, from which we obtain the time-dependent current fluctuation correlations, and consequently the spectral density of shot noise. The photon-assisted shot noise exhibits interesting behaviors due to the special properties of the TCN and the transport behaviors of electrons in multichannel mesoscopic systems. The quantum steps of the shot noise with respect to the source-drain bias reflect the quantum nature of the TCN, as well as the applied microwave field. The saturated value of the shot noise is suppressed by the applied microwave fields, and the suppression is strongly associated with the structure of the TCN. The obtained shot noises are sub-Poissonian when the source-drain bias increases to a definite value, and super-Poissonian shot noise appears below this value.

DOI: 10.1103/PhysRevB.74.245401 PACS number(s): 73.23.−b, 85.35.−p, 72.25.Mk, 73.21.La

I. INTRODUCTION

In mesoscopic systems, electrons travel through the sample maintaining coherence of the single-particle wave function. The current $I(t)$ tunneling through a conductor may fluctuate in time even under constant operation conditions. The noise is usually characterized by its power spectrum at frequency ω, and it is defined as the Fourier transform of the current correlation function.[1,2] It is well known that for a conventional macroscopic dissipative conductor at equilibrium there exists a generalized Nyquist current noise spectral density[3] $P(\omega)=4G\varepsilon(\omega,T)$, where $\varepsilon(\omega,T)$ is the energy of a harmonic oscillator, and G is the conductance of the conductor. It is well known that there are two types of equilibrium fluctuations: Johnson-Nyquist noise[4] due to random motion of the charged carriers, and the noise due to time-dependent fluctuations in the resistance. The shot noise is a nonequilibrium fluctuation which is caused by the discreteness of charged carriers.[5–7] From the investigation of shot noise, we can learn additional information about the electronic structure and transport properties, since the shot noise is directly related to the degrees of randomness in carrier transfer. Investigation of the deviations from purely Poissonian shot noise in mesoscopic systems has been an increasingly interesting subject. Due to the Poissonian distribution in a macroscopic system, the current is related to the shot noise by the well-known Schottky formula[8] $S_P=2e\langle I\rangle$. However, for a mesoscopic system, the electrons are correlated due to coherent transport, and they are governed by the Fermi distribution and the Pauli principle. The Pauli suppression of shot noise has been demonstrated experimentally by several groups.[9–12] The shot noise suppression in the one-dimensional hopping model[13] and suppression by the Fermi and Coulomb interactions[14] have been discussed. The enhanced shot noise was derived theoretically by considering a diode-biased resonant tunneling system in the negative differential resistance regions.[15] The enhancement of shot noise was observed in the case of resonant tunneling via localized states.[16]

Carbon nanotubes (CNs) are prospective materials for future electronic devices due to their metallic and semiconducting behaviors. Some electronic devices like field effect transistors[17,18] and diodes[19] have been fabricated, which have great potential for application. This opens up a new artificial laboratory to study transport properties of low-dimensional systems, and provides physical predictions for further device application.[20–26] The toroidal carbon nanotube (TCN) is a form of carbon structure that has a torus structure formed by bending the carbon tube such that the two edges are connected. Theoretical[27–29] and experimental[30] investigations of the electron properties of the carbon toroid revealed the quantum nature of the quasi-one-dimensional ring. Compared with a normal-metal or semiconductor ring, the TCN can carry a larger persistent current due to the modification of the energy structure and energy gap,[31] and it provides much richer physical properties due to its structure. Many properties such as the conductance of a TCN coupled with normal metals (N-TCN-N), Andreev reflection in a TCN coupled to a normal metal and a superconductor (N-TCN-S), and the dc Josephson current through a system with a TCN coupled to two superconducting leads (S-TCN-S) (Ref. 32) have been investigated and show novel electronic transport properties. For a TCN that is threaded with a static magnetic flux ϕ, the interference of the electrons traversing different arms of the ring induces Aharonov-Bohm-like effects. The conductance and tunneling current are found to show resonant and oscillating behaviors associated with magnetic flux. The Aharonov-Bohm-like magnetic flux controls the tunneling current since it causes the metal-semiconductor transition in the TCN.[33] In the previous work, we have investigated photon-assisted mesoscopic transport through the N-TCN-N system by imposing microwave fields on metal leads, and by

considering a terahertz (THz) magnetic flux threaded through a TCN.[34,35]

In this paper, we investigate the photon-assisted shot noise in a mesoscopic system with a TCN coupled to two normal-metal leads perturbed by ac fields. The tunneling current is characterized by the oscillating features of the external microwave field. The external microwave fields split the transmission channels to form sidebands, and drive electrons resonantly in the TCN. In the presence of ac fields, the tunneling features deviate from those in situations where there are no time-dependent perturbations.[36–40] This is because time-reversal symmetry is broken due to the ac disturbance. We find that the tunneling current strongly depends on the structure of the TCN and the applied fields, and the multichannel transport behaviors are determined by the detailed structure of the TCN and the sideband of photon irradiations. We derive the photon-assisted tunneling current operator by using the method of the equation of motion. The corresponding photon-assisted shot noise spectral density is obtained by studying the current correlation functions. The shot noise formula is found to be similar to the Büttiker formula[37] by using scattering theory. Since the energy level differences of the TCN are larger as the TCN gets smaller, we consider applied microwave fields located in the THz regime. Although a similar formula for the shot noise in the presence of photon-assisted tunneling in a single-level quantum dot system has been presented in Ref. 39, our study displays unusual physical properties due to the detailed specific electronic structure of the TCN.

II. HAMILTONIAN AND FORMALISM

The TCN is formed by rolling a finite graphite sheet from the origin to the vectors $\mathbf{R}_x=m_1\mathbf{a}_1+m_2\mathbf{a}_2$, and $\mathbf{R}_y=p_1\mathbf{a}_1+p_2\mathbf{a}_2$ simultaneously, where $\mathbf{a}_1$ and $\mathbf{a}_2$ are the two primitive lattice vectors possessing the same magnitude as $a=|\mathbf{a}_1|=|\mathbf{a}_2|=b\times 3^{1/2}$. Here $b=1.44$ Å is the C-C bond length of CNs, known to be slightly larger than that of graphite.[41] We denote the TCNs by $(m_1,m_2;p_1,p_2)$ as convention. The TCN satisfies the periodical boundary conditions along both of the longitudinal and transverse directions. Two kinds of TCN with highly symmetric structures are the armchair $(m,m;-p,p)$ TCN and the zigzag $(m,0;-p,2p)$ TCN. The armchair TCN possesses symmetry with the armchair structure along the transverse direction and zigzag structure along the longitudinal direction. The zigzag TCN has zigzag structure in both directions. We denote the diameter of the CN as d_t, and the diameter of the mesoscopic ring as D_t. The diameters of the armchair $(m,m;-p,p)$ TCN are $d_t=3bm/\pi$, and $D_t=3^{1/2}bp/\pi$; the diameters of the zigzag $(m,0;-p,2p)$ are given by $d_t=3^{1/2}bm/\pi$, and $D_t=3bp/\pi$. In the absence of magnetic flux, the armchair TCN is a metal when $p=3\nu$ (type I TCN), while it is a semiconductor with narrow energy gap when $p=3\nu\pm1$ (type II TCN), where ν is an integer. The zigzag TCN exhibits semiconductor behavior with large energy gap of the order $E_g=0.1-1.0$ eV, and is referred to as a type III TCN. We investigate a system with the diameter ratio of the nanotube d_t to the diameter D_t of the mesoscopic ring being much smaller than 1, i.e., $\kappa=d_t/D_t\ll1$. In the absence of magnetic flux, the energy gap of the type II TCN can be calculated by $E_g=2\gamma_0|1-z(\xi)|$, where $z(\xi)=\cos(\xi)-3^{1/2}\sin(\xi)$, and $\xi=b/(3^{1/2}D_t)$.[32,33] The energy gap of the $(7,7;-160,160)$ TCN is calculated to be $E_g\approx68.77$ meV.

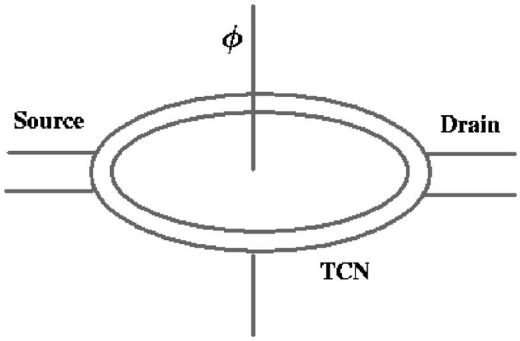

FIG. 1. Schematic diagram of a TCN coupled to two normal metal leads. The TCN is well connected to the two leads which serve as the source and drain. The ac fields are applied to the two leads to induce ac bias voltage.

Our system consists of three parts: the central TCN, and two normal metal leads. The central TCN is applied with a static magnetic field **B** perpendicular to the ring, which induces a magnetic flux ϕ threaded through the TCN. The electrons are free from the magnetic field **B**, but the vector potential **A** affects the behaviors of electrons due to the Aharonov-Bohm effect. The electrons of the leads are described by the grand canonical ensemble, and the central TCN is described by the tight-binding Hamiltonian. The microwave field with frequency ω is applied to the γth lead forming the potential drops by $e\tilde{V}_{\gamma d}\cos(\omega t)$, so that the electron energy in the γth lead is associated with the time-dependent one $\epsilon_{\gamma k}(t)=\epsilon_{\gamma k}^{(0)}+e\tilde{V}_{\gamma d}\cos(\omega t)$. We show the geometric structure of our system in Fig. 1 in order to understand it graphically. We consider the circumstance that the two leads are biased by the dc voltage V which equals the chemical potential drop between the two leads as $\mu_L-\mu_R=eV$. In the diagonalized representation of the TCN, the electronic properties can be determined by the total Hamiltonian of the system, which is the summation of the three sub-Hamiltonians and the tunneling interaction term[34]

$$H=\sum_{\gamma k\sigma}\epsilon_{\gamma k}(t)a_{\gamma,k\sigma}^{\dagger}a_{\gamma,k\sigma}+\sum_{j\ell\delta\sigma}E_{\delta,\ell j}(\phi)c_{\delta\sigma,j\ell}^{\dagger}c_{\delta\sigma,j\ell}+\sum_{\gamma k\sigma}\sum_{j\ell\delta}[R_{\gamma\delta,j\ell}^{*}c_{\delta\sigma,j\ell}^{\dagger}a_{\gamma,k\sigma}+\text{H.c.}],\quad(1)$$

where $a_{\gamma,k\sigma}^{\dagger}$ ($a_{\gamma,k\sigma}$) and $c_{\delta\sigma,j\ell}^{\dagger}$ ($c_{\delta\sigma,j\ell}$) are the creation (annihilation) operators of electron in the two leads and the TCN, respectively. $R_{\gamma\delta,j\ell}(k)$ is the interaction strength of particles between the γth lead and the TCN. In the Hamiltonian Eq. (1), $E_{\delta,\ell j}(\phi)$ is the energy of the TCN, which is closely related to the structure of a specific TCN. The energy of the armchair TCN in tight-binding approximation is given by[31]

$$E_{\delta,\ell j}(\phi) = \delta\gamma_0\left[1 + 4\cos\left(\frac{\pi j}{m}\right)\cos\left(\frac{\pi(\ell + \phi/\phi_0)}{p}\right) + 4\cos^2\left(\frac{\pi(\ell + \phi/\phi_0)}{p}\right)\right]^{1/2}. \quad (2)$$

The energy of the zigzag TCN in the tight-binding approximation is given by

$$E_{\delta,\ell j}(\phi) = \delta\gamma_0\left[1 + 4\cos\left(\frac{\pi j}{m}\right)\cos\left(\frac{\pi(\ell + \phi/\phi_0)}{p}\right) + 4\cos^2\left(\frac{\pi j}{m}\right)\right]^{1/2}, \quad (3)$$

where $j=1,2,\ldots,m$; $\ell=1,2,\ldots,2p$; $\delta=\pm$, $\gamma_0=3.033$ eV, and $\phi_0=h/e$ is the flux quantum. j and ℓ are the quantum numbers of energy describing the transverse and longitudinal quantization of the TCN, respectively. The upper half of the energy dispersion curves expresses the π^*-energy antibonding band (unoccupied state), and the lower half of the energy dispersion curves describes the π-energy bonding band (occupied state).

In order to investigate the shot noise of our system, we first find the time-dependent current operator, and then consider the current fluctuation correlations at different times. It is convenient to make the gauge transformation over the Hamiltonian by letting $\Psi(t)=\hat{U}(t)\tilde{\Psi}(t)$ in the Schrödinger equation. The unitary operator is defined by $\hat{U}(t)=\exp[-i\Sigma_{\gamma k\sigma}\lambda_\gamma a^\dagger_{\gamma,k\sigma}a_{\gamma,k\sigma}\sin(\omega t)]$, with $\lambda_\gamma=e\tilde{V}_{\gamma d}/(\hbar\omega)$. The transformed Hamiltonian $\tilde{H}=\hat{U}^{-1}(t)H\hat{U}(t)$ is obtained simply by letting $\epsilon_{\gamma k}(t)\to\epsilon^{(0)}_{\gamma k}$ and $R_{\gamma\delta,j\ell}\to\tilde{R}_{\gamma\delta,j\ell}(t)=R_{\gamma\delta,j\ell}\exp[i\lambda_\gamma\sin(\omega t)]$ in Eq. (1). This procedure indicates that the gauge transformation transforms the time-dependent term in the electron energies $\epsilon_{\gamma k}(t)$ to the tunneling interaction terms $\tilde{R}_{\gamma\delta,j\ell}(t)$.

The tunneling current operator of the γth lead is determined from the Heisenberg equation and continuity equation. Substituting the gauge-transformed Hamiltonian $\tilde{H}(t)$ into the definition of current, the current operator is expressed by the creation and annihilation operators of electrons in the normal metal leads and the TCN as

$$\hat{I}_\gamma(t) = -\frac{ie}{\hbar}\sum_{j\ell\delta}\sum_{k\sigma}[\tilde{R}^*_{\gamma\delta,j\ell}(t)c^\dagger_{\delta\sigma,j\ell}(t)a_{\gamma,k\sigma}(t) - \tilde{R}_{\gamma\delta,j\ell}(t)a^\dagger_{\gamma,k\sigma}(t)c_{\delta\sigma,j\ell}(t)]. \quad (4)$$

Due to the coupling of different parts of the subsystems and the time-dependent perturbation, the electrons in the leads and the TCN are in nonequilibrium states, which are determined by the time-dependent electron operators $a^\dagger_{\gamma,k\sigma}(t)$, $a_{\gamma,k\sigma}(t)$ and $c^\dagger_{\delta\sigma,j\ell}(t)$, $c_{\delta\sigma,j\ell}(t)$. The shot noise is determined by the current correlation as

$$\Pi_{\gamma\gamma'}(t,t') = \langle\delta\hat{I}_\gamma(t)\delta\hat{I}_{\gamma'}(t')\rangle + \langle\delta\hat{I}_{\gamma'}(t')\delta\hat{I}_\gamma(t)\rangle, \quad (5)$$

where $\delta\hat{I}_\gamma(t)=\hat{I}_\gamma(t)-\langle\hat{I}_\gamma(t)\rangle$. The symbol $\langle\cdots\rangle$ in the above formula denotes the quantum expectation over the electronic state, and the ensemble average over the system. In order to obtain the shot noise, one has to find the current operator explicitly. We derive the electron operators by solving the equation of motion in the Heisenberg picture. The electron operator in the γth lead for the coupled system is expressed as the integral form

$$a_{\gamma,k\sigma}(t) = \int dt_1 g^r_{\gamma,k\sigma}(t,t_1)\sum_{j\ell\delta}\tilde{R}_{\gamma\delta,j\ell}(t_1)c_{\delta\sigma,j\ell}(t_1) + \hat{a}_{\gamma,k\sigma}(t), \quad (6)$$

where $\hat{a}_{\gamma,k\sigma}(t)$ is the annihilation operator of electron in the γth lead when there is no tunneling at the initial time t_0. This means that $\hat{a}_{\gamma,k\sigma}(t)$ describes the equilibrium state of electron as $\tilde{R}_{\gamma\delta,j\ell}(t_1)=0$. We refer to it as $\hat{a}_{\gamma,k\sigma}(t)=\exp[-(i/\hbar)\epsilon^{(0)}_{\gamma k}(t-t_0)]\hat{a}_{\gamma,k\sigma}(t_0)$. The electron number in the leads satisfies the Fermi distribution $\langle\hat{a}^\dagger_{\gamma,k\sigma}(t)\hat{a}_{\gamma,k\sigma}(t)\rangle=f(\epsilon^{(0)}_{\gamma k})$. The retarded Green's function of the γth lead is denoted as $g^r_{\gamma,k\sigma}(t,t_1)$. We still need the definition of the time-dependent electron operator in the TCN $c_{\delta\sigma,j\ell}(t_1)$ in order to find the solution of $a_{\gamma,k\sigma}(t)$. One can find that the nonequilibrium electron operator of the TCN is determined by solving the Heisenberg equation to give in the integral form

$$c_{\delta\sigma,j\ell}(t) = \sum_{\gamma k}\int dt_1 g^r_{\delta\ell j}(t,t_1)\tilde{R}^*_{\gamma\delta,j\ell}(t_1)a_{\gamma,k\sigma}(t_1) + \hat{c}_{\delta\sigma,j\ell}(t), \quad (7)$$

where $g^r_{\delta\ell j}(t,t_1)$ is the retarded Green's function of the isolated TCN, and $\hat{c}_{\delta\sigma,j\ell}(t)$ is the electron operator of the isolated TCN defined by $\hat{c}_{\delta\sigma,j\ell}(t)=\exp[-(i/\hbar)E_{\delta,\ell j}(\phi)(t-t_0)]\hat{c}_{\delta\sigma,j\ell}(t_0)$. The initial electron operator $\hat{c}_{\delta\sigma,j\ell}(t)$ of the TCN can be neglected since it has no contribution to the current for our system. This is also true for the shot noise due to the fact that there exists no correlation between the initial operators $\hat{a}_{\gamma,k\sigma}(t)$ and $\hat{c}_{\delta\sigma,j\ell}(t)$. We consider the interaction of electrons only in the same channels, i.e., $\tilde{R}^*_{\gamma\delta,j\ell}(t)\tilde{R}_{\gamma\delta_1,j_1\ell_1}(t')=\tilde{R}^*_{\gamma\delta,j\ell}(t)\tilde{R}_{\gamma\delta,j\ell}(t')\delta_{\delta\delta_1}\delta_{jj_1}\delta_{\ell\ell_1}$, which means the self-energy of electrons in the γth lead $\Sigma^r_{\gamma\delta,j\ell}(t,t')=\Sigma_k\tilde{R}^*_{\gamma\delta,j\ell}(t)\tilde{R}_{\gamma\delta j\ell}(t')g^r_{\gamma,k\sigma}(t,t')$. Combining Eqs. (6) and (7), and employing the iteration procedure, we can find the electron operator

$$c_{\delta\sigma,j\ell}(t) = \sum_{\gamma k}\int dt_1 G^r_{\delta\ell j}(t,t_1)\tilde{R}^*_{\gamma\delta,j\ell}(t_1)\hat{a}_{\gamma,k\sigma}(t_1). \quad (8)$$

In the above equation we have dropped the contribution of the initial electron operator $\hat{c}_{\delta\sigma,j\ell}(t)$ of the TCN. In the electron operator $c_{\delta\sigma,j\ell}(t)$ above, we have introduced the retarded Green's function $G^r_{\delta\ell j}(t,t_1)$ of the coupled TCN, which is determined by the Dyson equation. Substituting the operator $c_{\delta\sigma,j\ell}(t)$ given in Eq. (8) into Eq. (6), we therefore obtain the electron operator $a_{\gamma,k\sigma}(t)$. The conjugate operator of $c_{\delta\sigma,j\ell}(t)$ can be found by taking conjugation over Eq. (8), and by using the relation $G^{r*}_{\delta\ell j}(t,t_1)=G^a_{\delta\ell j}(t_1,t)$ of the retarded and advanced Green's functions. This means that the electron operators in the nonequilibrium state can be expressed by the

nonequilibrium Green's functions and the electron operators in equilibrium state. From Eq. (8) and its conjugate expression, one can derive an expression for the product of $c^{\dagger}_{\delta\sigma,j\ell}(t)$ and $c_{\delta\sigma,j\ell}(t)$ to describe the nonequilibrium electron population operator in the TCN, from which we can obtain the electron number in the TCN by taking quantum average and ensemble average.

The current operator formula is obtained from Eq. (4) by substituting all of the required equations above. In the wideband limit, $R_{\gamma\delta,j\ell}$ is a constant, and does not depend on the concrete energy levels. We denote it as $R_{\gamma\delta,j\ell}=R_{\gamma}$. The linewidth function $\Gamma_{\gamma\beta}=2\pi\Sigma_k R^{*}_{\gamma}R_{\beta}\delta(\epsilon-\epsilon^{(0)}_{\gamma k})$ becomes an energy-independent constant in the wideband limit. After straightforward calculation, the time-dependent current operator is found to be

$$\hat{I}_{\gamma}(t)=\frac{e}{h}\sum_{\delta\ell j}\sum_{mn\sigma}\sum_{\beta\beta'}\int\int d\epsilon_1 d\epsilon_2 J_m(\lambda_{\beta'})J_n(\lambda_{\beta}) \times \exp\left(\frac{i}{\hbar}\varepsilon^{nm}_{12}t\right)A^{\gamma}_{\beta\beta',mn}(\epsilon_1,\epsilon_2)\hat{a}^{\dagger}_{\beta\sigma}(\epsilon_1)\hat{a}_{\beta'\sigma}(\epsilon_2), \quad (9)$$

where $\varepsilon^{nm}_{ij}=\epsilon_i-\epsilon_j+(n-m)\hbar\omega$, and $J_n(\lambda)$ is the Bessel function of the first kind. We have defined the transmission function of the time-dependent system by

$$A^{\gamma}_{\beta\beta',mn}(\epsilon_1,\epsilon_2)=-\Gamma_{\gamma\beta}\Gamma_{\beta'\gamma}G^{a}_{\delta\ell j}(\epsilon_1+n\hbar\omega)G^{r}_{\delta\ell j}(\epsilon_2+m\hbar\omega) + i\delta_{\beta\gamma}\Gamma_{\beta'\beta}G^{r}_{\delta\ell j}(\epsilon_2+m\hbar\omega) - i\delta_{\beta'\gamma}\Gamma_{\beta'\beta}G^{a}_{\delta\ell j}(\epsilon_1+n\hbar\omega).$$

The transmission function $A^{\gamma}_{\beta\beta',mn}(\epsilon_1,\epsilon_2)$ in the current operator satisfies the relation $A^{\gamma}_{\beta\beta',mn}(\epsilon_1,\epsilon_2)=A^{\gamma*}_{\beta'\beta,nm}(\epsilon_2,\epsilon_1)$. The retarded (advanced) Green's function of the coupled TCN system in energy space is obtained by solving the Dyson equation to give $G^{r(a)}_{\delta\ell j}(\epsilon)=1/[\epsilon-E_{\delta,\ell j}(\phi)\pm i\Gamma/2]$, where $\Gamma=\Sigma_{\gamma}\Gamma_{\gamma}$ represents the summation of the linewidth constant in the wideband limit for the two leads, with the notation $\Gamma_{\gamma}=\Gamma_{\gamma\gamma}$. From Eq. (9) we can derive the tunneling current $I_{\gamma}(t)=\langle\hat{I}_{\gamma}(t)\rangle$ by taking the ensemble and quantum average. By taking the grand canonical ensemble average over Eq. (9), and employing the relation $\langle\hat{a}^{\dagger}_{\beta\sigma}(\epsilon_1)\hat{a}_{\beta'\sigma'}(\epsilon_2)\rangle=\delta_{\sigma\sigma'}\delta_{\beta\beta'}\delta(\epsilon_1-\epsilon_2)f_{\beta}(\epsilon_1)$, we have the time-dependent current formula in the γth lead,

$$I_{\gamma}(t)=\frac{e}{h}\sum_{\delta\ell j}\sum_{mn\sigma}\sum_{\beta}\int d\epsilon\, J_m(\lambda_{\beta})J_n(\lambda_{\beta}) \times e^{i(n-m)\omega t}A^{\gamma}_{\beta\beta,mn}(\epsilon,\epsilon)f_{\beta}(\epsilon), \quad (10)$$

where the Fermi distribution function of the βth lead is given by $f_{\beta}(\epsilon)=1/\{\exp[(\epsilon-\mu_{\beta})/k_BT]+1\}$. This formula describes the time-oscillating mesoscopic transport through the TCN system in the presence of ac fields. The structure of the oscillating tunneling current is strongly associated with the ac fields, as well as the coupled TCN system. Experimentally, the observed tunneling current is associated with the time-averaged characteristics. The time-averaged tunneling current is given by taking the time average over Eq. (10), which is obtained simply by letting $n=m$ in the formula. The current conservation $\Sigma_{\gamma}I_{\gamma}=0$ is satisfied for the time-averaged current. The photon-assisted tunneling takes place as the applied ac fields induce sidebands for electrons to tunnel through the channels $\epsilon=E_{\delta,\ell j}(\phi)-n\hbar\omega$, $(n=0,\pm1,\pm2,\ldots)$. The photon-electron pumping effect takes place when the magnitudes of the ac fields are not equal, i.e., $\lambda_L\neq\lambda_R$, in the absence of dc bias. This means that as the source-drain bias is zero, there may exist a tunneling current due to the photon absorption effect for electrons to overcome the threshold in the TCN system. As the magnitudes of the applied ac fields are equal, i.e., $\lambda_L=\lambda_R=\lambda$, the tunneling current is zero when the source-drain bias is removed. This results from the fact that the pumped electrons from the two leads to the TCN are equal because of the equal ac biases. The energy gap alternates with ϕ, and the metal-semiconductor transition takes place on varying the magnetic flux. Therefore, the magnetic flux controls the energy gap $E_g(\phi)$ for forming periodic oscillation of current with respect to ϕ in period ϕ_0. The sidebands of photon energy also shift the energy threshold up and down to modify the energy gap. If $\hbar\omega$ is large enough to smear the energy gap for the electron to tunnel, the effective semiconductor-metal transition takes place.

The fluctuation of the time-dependent current associated with the correlations of γ and γ' leads at times t and t' is now can be completely solved by substituting Eq. (9) into Eq. (5). The current correlation contains the correlations of four electron operators $\hat{a}^{\dagger}_{\beta_1\sigma_1}(\epsilon_1)$, $\hat{a}_{\beta_2\sigma_2}(\epsilon_2)$, $\hat{a}^{\dagger}_{\beta_3\sigma_3}(\epsilon_3)$, $\hat{a}_{\beta_4\sigma_4}(\epsilon_4)$ for the isolated leads in equilibrium states. We employ Wick's theory to decompose the four operator correlations into the products of two operators with one creation and one annihilation operator. As a result, the current correlation $\Pi_{\gamma\gamma'}(t,t')$ between γ and γ' leads at times t and t', respectively, is derived as

$$\Pi_{\gamma\gamma'}(t,t')=\left(\frac{e}{h}\right)^2\sum_{\delta\ell j}\sum_{\delta'\ell'j'}\sum_{mnm'n'}\sum_{\beta\beta'\sigma}\int\int d\epsilon_1 d\epsilon_2 J_m(\lambda_{\beta'}) \times J_n(\lambda_{\beta})J_{m'}(\lambda_{\beta})J_{n'}(\lambda_{\beta'}) \times\exp\left(\frac{i}{\hbar}\varepsilon^{nm}_{12}t\right)\exp\left(\frac{i}{\hbar}\varepsilon^{n'm'}_{21}t'\right) \times A^{\gamma}_{\beta\beta',mn}(\epsilon_1,\epsilon_2)A^{\gamma'}_{\beta'\beta,m'n'}(\epsilon_2,\epsilon_1)F_{\beta\beta'}(\epsilon_1,\epsilon_2), \quad (11)$$

where we have defined the notation $F_{\beta\beta'}(\epsilon_1,\epsilon_2)=f_{\beta}(\epsilon_1)[1-f_{\beta'}(\epsilon_2)]+f_{\beta'}(\epsilon_2)[1-f_{\beta}(\epsilon_1)]$. The function $F_{\beta\beta'}(\epsilon_1,\epsilon_2)$ satisfies the symmetry relation $F_{\beta\beta'}(\epsilon_1,\epsilon_2)=F_{\beta'\beta}(\epsilon_2,\epsilon_1)$. This expression of current correlation indicates that the currents tunneling through the mesoscopic system are correlated not only between the currents in the same leads and times, but also between different leads and times. The correlations of electrons tunneling through different channels of the TCN and sidebands are also involved in the formula. Therefore, time-dependent current noise is contributed by the structure of the TCN, and by all of these correlations stated above. The features of the microwave fields play an important role in the current noise. Usually, we are interested in the spectral den-

sity of current noise $S_{\gamma\gamma'}(\Omega)$ in the pseudoequilibrium state, which is defined as the Fourier-transformed current correlation function of Eq. (5) by the expression shown in Ref. 5, $S_{\gamma\gamma'}(\Omega)\delta(\Omega+\Omega')=(1/2\pi)\Pi_{\gamma\gamma'}(\Omega,\Omega')$. Making a Fourier transformation over t and t' corresponding to the frequencies Ω and Ω' in $\Pi_{\gamma\gamma'}(t,t')$, and considering the pseudoequilibrium state in the presence of ac fields, we find the spectral density of current noise. The effect of photon absorption and emission induced by the microwave fields is included in the noise spectral density. In order to obtain the observed noise spectral density, the absorption and emission of photon numbers are required to satisfy the constraint $n-m+n'-m'=0$. This constraint comes from the requirement of Fourier transformation of the current correlation function in the pseudoequilibrium state. In fact, it is the selection rule for the absorption and emission of photons associated with the energy conservation, i.e., the total absorbed photon energy equals the total emitted photon energy in the system. This equation indicates the two cases that we will study: case I for $n=m$, $n'=m'$, which we refer to balanced absorption; case II for $m'=n-m+n'$, which we refer to as unbalanced absorption.

A. Balanced absorption

For simplicity, we consider a symmetric situation for the ac fields by letting $\lambda_L=\lambda_R=\lambda$. The noise spectral density for the balanced absorption case is determined by the formula

$$S_{\gamma\gamma'}(\Omega)=\frac{e^2}{h}\sum_{\delta\ell j}\sum_{\delta'\ell'j'}\sum_{nn'}\sum_{\beta\beta'\sigma}\int d\epsilon J_n^2(\lambda)J_{n'}^2(\lambda)\times A^{\gamma}_{\beta\beta',nn}(\epsilon,\epsilon+\hbar\Omega)A^{\gamma'}_{\beta'\beta,n'n'}(\epsilon+\hbar\Omega,\epsilon)\times F_{\beta\beta'}(\epsilon,\epsilon+\hbar\Omega). \tag{12}$$

Equation (12) describes the current noise spectral density, which contains the thermal noise and shot noise in the presence of ac fields. When the ac fields are weak, the major contribution to the noise comes from a few photon-assisted processes. For the balanced absorption situation, the absorptions and emission of photons in the same lead are equal, and there is no correlation between the sidebands of photon between currents in different leads.

Now we investigate the shot noise of the left lead by considering the special case as $\gamma,\gamma'=L$ in Eq. (12) for $\Omega=0$, i.e., $S=S_{LL}(0)$. This noise spectral density is originated from the self-correlations of the tunneling current in the same leads. From Eq. (12) and substituting the coefficients $A^{\gamma}_{\beta\beta',nn}$ defined in Eq. (9) into the spectral density of noise formula, one finally arrives at the noise expressed by the transmission coefficient $T^{LR}_{\delta'\ell'j'}(\epsilon)$ in the following form:

$$S=4\frac{e^2}{h}\sum_{\delta\ell j}\sum_{\delta'\ell'j'}\sum_{nn'}\int d\epsilon J_n^2(\lambda)J_{n'}^2(\lambda)T^{LR}_{\delta\ell j}(\epsilon+n\hbar\omega)\times T^{LR}_{\delta'\ell'j'}(\epsilon+n'\hbar\omega)\Bigg(\sum_{\beta\in\{L,R\}}f_\beta(\epsilon)[1-f_\beta(\epsilon)]+W^{(n,n')}_{\delta\ell j,\delta'\ell'j'}(\epsilon)F_{LR}(\epsilon,\epsilon)\Bigg). \tag{13}$$

In the noise formula, $T^{LR}_{\delta\ell j}(\epsilon)=\Gamma_L\Gamma_R|G^r_{\delta\ell j}(\epsilon)|^2$ represents the transmission coefficient of an electron tunneling from the right lead to the left one, and it satisfies the symmetry relation $T^{LR}_{\delta\ell j}(\epsilon)=T^{RL}_{\delta\ell j}(\epsilon)$. We have used the notation $W^{(n,n')}_{\delta\ell j,\delta'\ell'j'}(\epsilon)=\{[\epsilon-E_{\delta,\ell j}(\phi)+n\hbar\omega][\epsilon-E_{\delta',\ell'j'}(\phi)+n'\hbar\omega]+(\Gamma/2)^2\}/(\Gamma_L\Gamma_R)-1$. The summation over spin variable σ contributes a factor 2 in our spin-degenerate system. The first term of Eq. (13) represents the thermal noise of the system, and the second term is the photon-assisted shot noise. As $\lambda\to 0$, the noise reduces to the case without microwave fields. Since the thermal noise comes from the equilibrium statistical property, it decreases to zero on reducing the temperature to zero. The shot noise is the excess noise as the temperature approaches zero. By taking the zero-temperature limit $T\to 0$, and employing the property of the Fermi distribution function, we obtain the photon-assisted shot noise

$$S=4\frac{e^2}{h}\sum_{\delta\ell j}\sum_{\delta'\ell'j'}\sum_{nn'}\left(\int_{eV<0}^{0}+\int_{0}^{eV>0}\right)d\epsilon J_n^2(\lambda)J_{n'}^2(\lambda)\times T^{LR}_{\delta\ell j}(\epsilon+n\hbar\omega)T^{LR}_{\delta'\ell'j'}(\epsilon+n'\hbar\omega)W^{(n,n')}_{\delta\ell j,\delta'\ell'j'}(\epsilon). \tag{14}$$

For our multichannel system, the shot noise is not completely determined by the transmission coefficient, since the cross-channel correlations contribute to the noise.

For the symmetric system where $\Gamma_L=\Gamma_R=\Gamma/2$, the photon-assisted spectral density of shot noise is simplified to the form

$$S=\frac{e^2}{h}\left(\int_{eV<0}^{0}+\int_{0}^{eV>0}\right)\mathcal{L}^2(\epsilon)d\epsilon. \tag{15}$$

This represents the positive results due to the self-correlation in the same lead, but there also exist cross-channel correlations. We have defined the function in the above formula for simplifying our expression

$$\mathcal{L}(\epsilon)=\sum_{\delta\ell jn}\mathcal{L}_{\delta\ell jn}(\epsilon),$$

and the function $\mathcal{L}_{\delta\ell jn}(\epsilon)$ is defined by

$$\mathcal{L}_{\delta\ell jn}(\epsilon)=J_n^2(\lambda)\frac{\Gamma[\epsilon-E_{\delta,\ell j}(\phi)+n\hbar\omega]}{[\epsilon-E_{\delta,\ell j}(\phi)+n\hbar\omega]^2+(\Gamma/2)^2}.$$

The shot noise spectral density presented in Eq. (15) is complicated due to the correlations of electrons tunneling in different channels of the TCN, as well as in the sideband channels induced by the perturbation of microwave fields. This complication can be observed by expanding the integrand $\mathcal{L}^2(\epsilon)$ among the tunneling channels as

$$\mathcal{L}^2(\epsilon)=4\sum_{\delta\ell jn}J_n^4(\lambda)T^{LR}_{\delta\ell j}(\epsilon+n\hbar\omega)[1-T^{LR}_{\delta\ell j}(\epsilon+n\hbar\omega)]+\sum_{\delta\ell jn\neq\delta'\ell'j'n'}\mathcal{L}_{\delta\ell jn}(\epsilon)\mathcal{L}_{\delta'\ell'j'n'}(\epsilon). \tag{16}$$

The first term in Eq. (16) is contributed by the self-correlations of electrons tunneling in the same channels

given by Büttiker *et al.*[5] for a contact system, while the second term represents the correlations of electrons tunneling in different channels, which are not involved in their formulas. The cross-channel correlations are much smaller compared with the self-correlations of electrons in the same channels. Furthermore, resonant transport through a mesoscopic system is the main behavior of tunneling electrons, and most properties of nano-devices are related to the resonant transport. For this situation, the second term disappears, and the remaining shot noise in the presence of ac fields is described by the transmission coefficient $T^{LR}_{\delta\ell j}(\epsilon+n\hbar\omega)$ entirely. It should be pointed out that this result is not restricted by the requirement of symmetric couplings.

It is interesting to study the variation of shot noise with respect to the source-drain bias, from which we can learn the behaviors of shot noise similar to the investigation of differential conductance. The differential shot noise spectral density versus source-drain bias voltage V of our system is determined by

$$\frac{dS}{dV} = \frac{e^3}{h}\{\mathcal{L}^2(eV>0) - \mathcal{L}^2(eV<0)\}. \tag{17}$$

This result tells us that when $eV>0$, the differential shot noise dS/dV is positive, while when $eV<0$, it is negative. However, the detailed structure of the differential shot noise spectral density is determined by the coupled TCN and ac fields.

B. Unbalanced absorption

For the case of unbalanced absorption, the spectral density of current noise is derived by considering the condition that the sidebands of photon may possess correlations in the same terminal currents, as well as in different terminal currents. Direct derivation results in

$$S_{\gamma\gamma'}(\Omega) = \frac{e^2}{h}\sum_{\delta\ell j}\sum_{\delta'\ell'j'}\sum_{nmn'}\sum_{\beta\beta'\sigma}\int d\epsilon J_m(\lambda_{\beta'})J_n(\lambda_\beta) \times J_{n'}(\lambda_{\beta'})J_p(\lambda_\beta)A^{\gamma}_{\beta\beta',mn}(\epsilon,\tilde{\epsilon}_{nm})A^{\gamma'}_{\beta'\beta,pn'}(\tilde{\epsilon}_{nm},\epsilon) \times F_{\beta\beta'}(\epsilon,\tilde{\epsilon}_{nm}), \tag{18}$$

where we have used the notations in the above formula with $p=n+n'-m$, and $\tilde{\epsilon}_{nm}=\epsilon+(n-m)\hbar\omega+\hbar\Omega$. Equation (18) contains all the information of our system in the presence of ac fields, as well as the magnetic flux for the unbalanced absorption situation. This case indicates that the absorption and emission of photons in the same terminal current are not necessarily equal, but the total absorption and emission of photons in the correlated currents are equal. This also means that the absorbed photons in a terminal current may be emitted from the other terminal currents due to the correlation of current effects. The current noise includes the thermal noise and shot noise, which are strongly related to the applied ac fields and the structure of the TCN. The noise is contributed from the current correlations in the same lead as well as different leads. It is also contributed by the correlations of current branches tunneling in the same and different channels. This form of current noise is given by Pedersen and Büttiker[37] from the scattering matrix approach for a mesoscopic conductor, and by Sun *et al.* from the equation of motion method[39] for a single-level quantum dot system. However, the application of their formulas to our TCN system is not straightforward due to the special structure of our multilevel system. Here we should point out that the formula of Pedersen and Büttiker in Ref. 37 involves multiple channels in different leads, and the leads are connected through a contact. An electron tunneling from a channel in one terminal directly to a channel in the other terminal. For our system, the transport of electrons is quite different due to the different central regime. The TCN provides a multiple channel for electrons to tunnel; scattering and interference may exist in the central regime. An electron may be ejected from a terminal to a channel of the TCN, and then merge to the other terminal. The correlations may exist in different channels of tunneling electrons in the same terminal and different terminals. An electron in one channel of the TCN may absorb photons to jump to another channel as the photon energy is larger than the energy spacing of the TCN. The electron may jump back to a lower level of the TCN by emitting photons.

We also consider the situation for symmetric magnitudes of ac fields by letting $\lambda_L=\lambda_R=\lambda$. The shot noise spectral density of the left lead $S=S_{LL}(0)$ is now derived as

$$S = 4\frac{e^2}{h}\sum_{\delta\ell j}\sum_{\delta'\ell'j'}\sum_{nmn'}\int d\epsilon J_m(\lambda)J_n(\lambda)J_{n'}(\lambda)J_p(\lambda) \times T^{LR}_{\delta\ell j}(\epsilon+n\hbar\omega)T^{LR}_{\delta'\ell'j'}(\epsilon+p\hbar\omega)\left(\frac{1}{2}\sum_{\beta\in\{L,R\}}F_{\beta\beta}(\epsilon,\tilde{\epsilon}_{nm}) + W^{(n,p)}_{\delta\ell j,\delta'\ell'j'}(\epsilon)F_{LR}(\epsilon,\tilde{\epsilon}_{nm})\right). \tag{19}$$

In the formula, the first term containing $F_{\beta\beta}(\epsilon,\tilde{\epsilon}_{nm})$ represents the thermal noise and shot noise in the presence of photon absorption and emission, which does not disappear in the presence of ac fields even at zero temperature. The second term represents the shot noise, which is nonzero when the source-drain bias is set to zero due to the absorption and emission of photons for the unbalanced situation. The dynamical current noise is obtained by setting the electrochemical potential of both leads to zero, i.e., $\mu_L=\mu_R=0$. For this case the current noise is contributed by the transmission noise between different terminals as well as the noise in the same terminals. At zero temperature the current noise is given by

$$S = 4\frac{e^2}{h}\sum_{\delta\ell j}\sum_{\delta'\ell'j'}\sum_{nmn'}J_m(\lambda)J_n(\lambda)J_{n'}(\lambda)J_p(\lambda) \times\left(\int_{(m-n)\hbar\omega<0}^{0} + \int_{0}^{(m-n)\hbar\omega>0}\right)T^{LR}_{\delta\ell j}(\epsilon+n\hbar\omega) \times T^{LR}_{\delta'\ell'j'}(\epsilon+p\hbar\omega)[1+W^{(n,p)}_{\delta\ell j,\delta'\ell'j'}(\epsilon)]d\epsilon, \tag{20}$$

where $p=n+n'-m$. The ac field perturbation on the leads causes two effects: one is to modify the electron energy levels of the TCN forming sidebands, and the other is that it

induces the photon bias energy which takes the role of the source-drain bias. The noise spectral density is contributed by four electron operators each of which represents an electron in the terminals. Unbalanced absorption indicates that absorption and emission of photons between every two electron operators are not necessarily equal, but the total absorption and emission of photons for the four electron operators are conserved. One notes that, for the symmetric ac-biased system where $\lambda_L=\lambda_R=\lambda$ and $\omega_L=\omega_R=\omega$, there is no net current when $eV=0$. However, the shot noise may not be zero for the unbalanced situation. In order to obtain nonzero shot noise, the condition $|m-n|\hbar\omega>\tilde{E}_g/2$ is required, where $\tilde{E}_g$ is the effective energy gap for our system. The effective energy gap means the photon-energy-modified energy gap which is not the same one as E_g for a TCN.

III. NUMERICAL CALCULATION AND RESULTS

In the following we perform the numerical calculations of shot noise S, differential shot noise dS/dV, and Fano factor $F=S/(2eI)$ versus source-drain bias eV, and photon energy. The symmetric system is studied by setting $\Gamma=2\Gamma_L=2\Gamma_R$ and $\lambda_L=\lambda_R=\lambda$. We perform the numerical calculations separately for the balanced and unbalanced photon absorption situations at zero temperature. The photon energy of the fields is scaled by the parameter γ_0 as $\hbar\omega=0.01\gamma_0$, which is related to the frequency in the microwave region as $\nu=7.36\times10^{12}$ Hz.

Figure 2(a) displays the shot noise spectral density of the type II (7,7;−74,74) TCN system at different strengths of microwave fields λ for the balanced photon absorption situation. A small energy gap is exhibited and step-like shot noise characteristics are seen on increasing the source-drain bias eV. This quantum step behavior comes from the discrete energy spectrum of the TCN and the sidebands induced by photon absorption. The shot noise changes abruptly at about $eV\approx0.44\gamma_0$. Applying the ac fields one observes that as the magnitude λ is increased, the shot noise is decreased. This kind of shot noise suppression comes from the effect of increasing the tunneling channels due to applying the ac fields, and the magnitude of the tunneling current is suppressed as a compensation for increasing the channel number. The magnitude of total tunneling current is also suppressed by the fields. The shot noise characteristic is strongly dependent on the structure of TCN shown in Fig. 2(b). A large energy gap is obviously seen for a type III (7,0;−75,150) TCN system, and there is no energy gap for the type I (7,7;−75,75) TCN system. The shot noise of type I TCN systems possesses a zero energy gap, and it behaves quite differently from type III TCN systems. The shot noise versus eV displays nonlinear characteristics for the different TCN systems.

The Fano factor tells us whether the shot noise is sub-Poissonian ($F<1$), or super-Poissonian ($F>1$). The detailed behavior of the Fano factor also presents the difference of the shot noise spectral density from corresponding current. Usually, the shot noise is suppressed in the positive conductance regime, but enhanced in the negative conductance regime. We show the variation of Fano factor versus source-drain bias eV in Fig. 3 at different system parameters for the balanced photon absorption situation. The curves shown in diagrams (a) and (b) are associated with the different (7,7;−74,74) and (7,7;−75,75) TCN systems when $\lambda=0.5$. We observe that at small eV, the Fano factors of the two systems behave quite differently. The Fano factor of the type II (7,7;−74,74) TCN drops rapidly to 0.25 as $eV=15$ meV. It rises rapidly to the value 0.59, and then it drops again. The Fano factor fluctuates around 0.4 when the source-drain bias eV is large enough for both (7,7;−75,75) and (7,7;−74,74) TCN systems. For the type I (7,7;−75,75) TCN $\lambda=0$, the Fano factor approaches the saturated value at about 0.5 when $eV\gg0.18\gamma_0$ as shown in diagram (c). The saturated value of the shot noise as well as the Fano factor are suppressed by the applied microwave field.

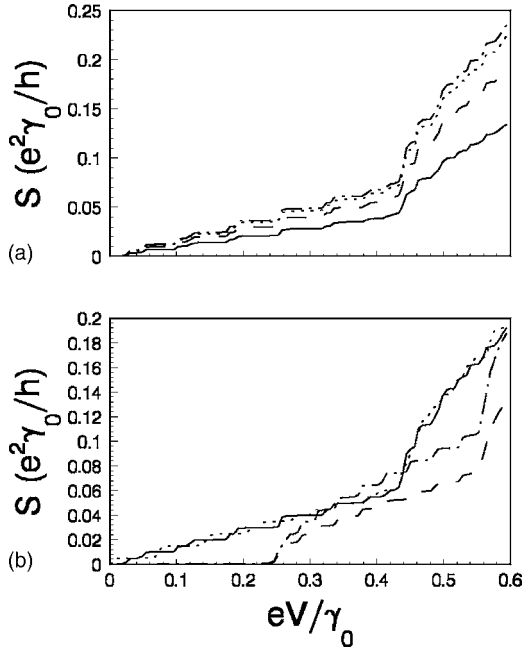

FIG. 2. Shot noise S versus source-drain bias eV at zero temperature for balanced absorption. We set the parameters as $\phi=0$, $\Gamma=0.001\gamma_0$, and $\hbar\omega=0.01\gamma_0$. (a) displays the case for (7,7;−74,74) with different ac field strengthes for $\lambda=0.8,0.5,0.3,0.2$ corresponding to the solid, dashed, dotted, and dash-dotted curves, respectively. (b) shows the shot noise for comparing different TCNs and λ. The solid, dotted, and dash-dotted curves are depicted associated with $\lambda=0.5$ corresponding to (7,7;−74,74), (7,7;−75,75), and (7,0;−75,150), respectively. The dashed curve is related to (7,0;−75,150) as $\lambda=0.8$.

In order to display the detailed resonant structure of dS/dV and the effects related to differential shot noise, we depict dS/dV in the small regime $|eV|<5\times10^{-2}\gamma_0$ in Fig. 4. Diagrams (a) and (b) display different behaviors of differential shot noise for the unbalanced and balanced absorption cases. For the unbalance absorption, dS/dV exhibits a Fano type of peak splitting behaviors with one peak and one valley asymmetry. This arises from the absorption of photons causing unbalanced behaviors of the emitting photons. For the balanced absorption case, resonant structures and the suppression of resonance caused by the microwave fields are clearly seen. We can only find the splitting of dS/dV, but the Fano-type asymmetry disappears. We also depict the differential conductance in diagram (c) for comparison. The small

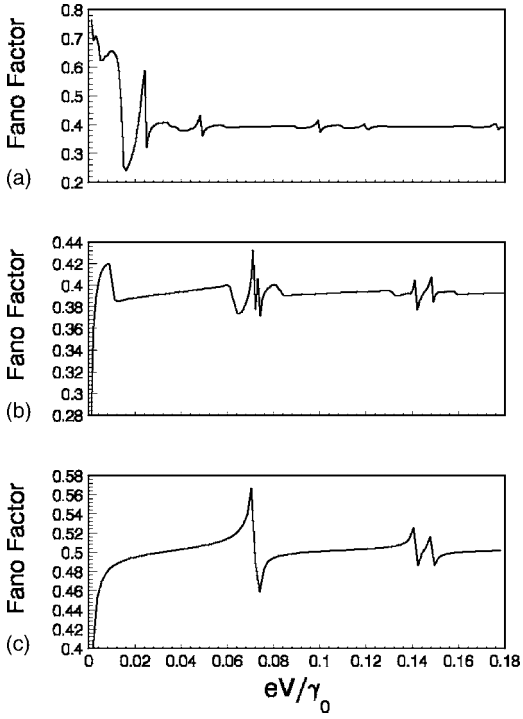

FIG. 3. Fano factor versus source-drain bias eV at zero temperature for balanced absorption. We set the parameters as $\phi=0$, $\Gamma=0.001\gamma_0$, and $\hbar\omega=0.01\gamma_0$. (a) is related to $(7,7;-74,74)$ as $\lambda=0.5$; (b) and (c) are related to $\lambda=0.5$ and 0, respectively, for $(7,7;-75,75)$.

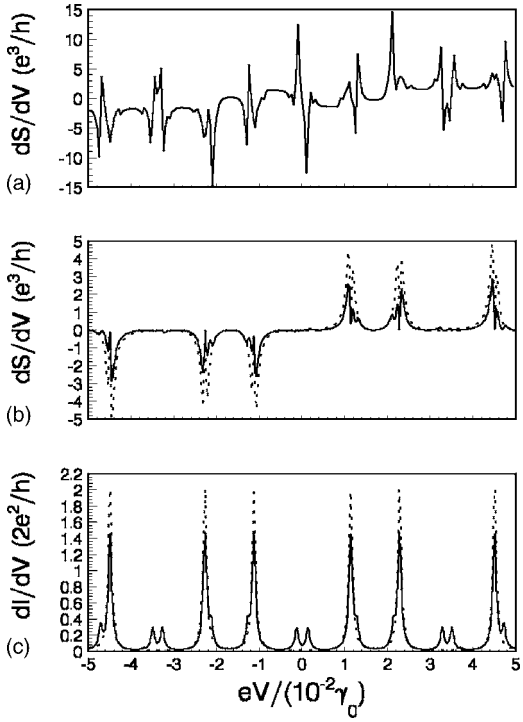

FIG. 4. Differential shot noise dS/dV and differential conductance dI/dV versus source-drain bias eV for $(7,7;-160,160)$. We set the parameters as $\phi=0$, $\Gamma=0.001\gamma_0$, and $\hbar\omega=0.01\gamma_0$. (a) displays the situation for unbalanced absorption as $\lambda=0.8$, while (b) shows the balanced absorptions for $\lambda=0.8$ (solid) and $\lambda=0$ (dotted). (c) shows the differential conductance $dI/dV-eV$ characteristics for comparison. The solid and dotted curves are associated with $\lambda=0.8$, $\lambda=0$, correspondingly.

energy gap $E_g\approx 2.26\times 10^{-2}\gamma_0$ of the type II $(7,7;-160,160)$ TCN in the absence of microwave fields is observed. This energy gap is also reflected in the resonant structure of the dS/dV shown in diagram (b). The energy gap disappears on applying a microwave field, which can be seen in the differential conductance by adding a split peak at $V=0$. However, we do not find the resonant peaks at $V=0$ in the structure of dS/dV for the balanced absorption case, which indicates that the behaviors of differential conductance are different from those of corresponding to differential shot noise.

We perform the numerical calculations of shot noise versus photon energy $\hbar\omega$ at zero temperature as $\tilde{V}_{\gamma d}=0.8\gamma_0$ for the unbalanced absorption case. To consider the behavior of shot noise associated with the photon energy we set magnetic flux to zero. We display the shot noise for $\Gamma=0.01\gamma_0$ at zero source-drain bias $V=0$ in Fig. 5. This kind of shot noise is induced by the applied ac fields entirely. One observes that the shot noise is zero as $\hbar\omega<0.08\gamma_0$ for the type I $(7,7;-75,75)$ and type II $(7,7;-74,74)$ TCNs, and in the regime $\hbar\omega<0.15\gamma_0$ for the type III $(7,0;-75,150)$ TCN. We denote $\Delta=0.08\gamma_0$ for $(7,7;-75,75)$ and $(7,7;-74,74)$ TCNs, and $\Delta=0.15\gamma_0$ for the $(7,0;-75,150)$ TCN. When $\hbar\omega>\Delta$, the shot noise increases rapidly as the photon energy increases. Steplike nonlinear behaviors are exhibited clearly, and they are intimately associated with the detailed electron structures of TCNs. This field-induced shot noise originates from several effects. First, the argument λ_γ of the Bessel functions is determined by $\lambda_\gamma=e\tilde{V}_{\gamma d}/(\hbar\omega)$, which is inversely propor-

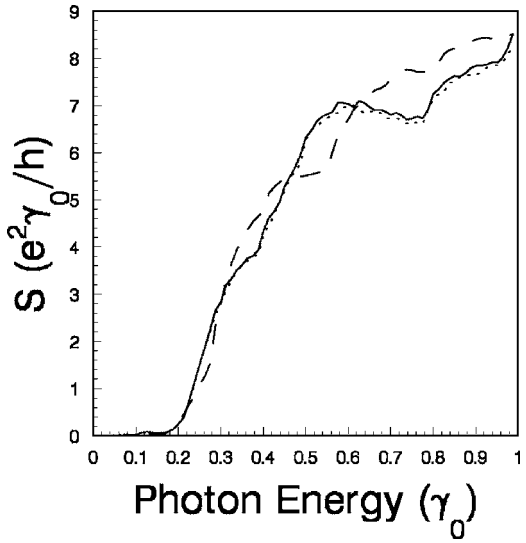

FIG. 5. Shot noise S of the unbalanced absorption case versus the photon energy $\hbar\omega$ at zero temperature as $eV=0$. The parameters are chosen as $\phi=0$, $e\tilde{V}_{\gamma d}=0.8\gamma_0$, and $\Gamma=0.01\gamma_0$. The solid, dotted, and dashed curves are related to the $(7,7;-75,75)$, $(7,7;-74,74)$, and $(7,0;-75,150)$ TCNs, respectively.

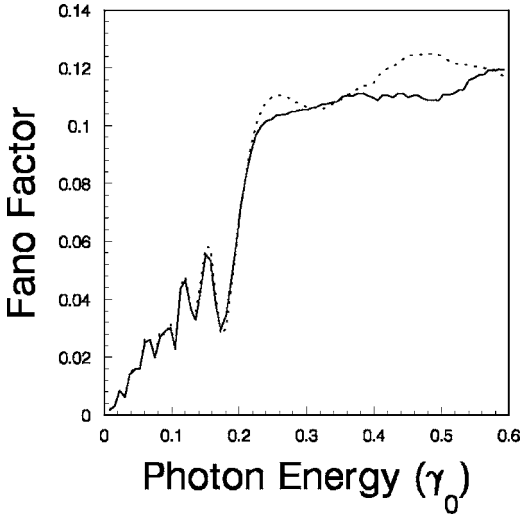

FIG. 6. Fano factor of the unbalanced absorption case at the source-drain bias $eV=0.25\gamma_0$ versus photon energy. The parameters are chosen as $\phi=0$, $e\tilde{V}_{\gamma d}=0.8\gamma_0$, and $\Gamma=0.001\gamma_0$. The solid and dotted curves are associated with $(7,7;-75,75)$, and $(7,0;-75,150)$ TCNs, respectively.

tional to $\hbar\omega$, so that the arguments of the Bessel functions are very large when the photon energy $\hbar\omega \ll \gamma_0$. There exists a photon-electron threshold Δ due to the ac fields and the nature of the TCNs. In order to obtain large shot noise, we have to increase the photon energy to force the tunneling electron to overcome the threshold $\hbar\omega > \Delta$. Second, the sidebands induced by the ac fields are incorporated with the energy levels of the TCN to form hybrid electron resonant levels. These energy levels enable electrons to tunnel through the system resonantly, and small steps are related to them. Since different TCNs possess different energy dispersion curves, we have different shot noise spectral density for different TCNs.

We perform numerical calculations of Fano factor versus photon energy $\hbar\omega$ at zero-temperature as $\tilde{V}_{\gamma d}=0.8\gamma_0$ for the unbalanced absorption case. Figure 6 depicts the Fano factor for $\Gamma=0.001\gamma_0$ in the presence of source-drain bias $eV=0.25\gamma_0$. The Fano factor is very small when the photon energy is small, and it increases to exhibit several resonant peaks in the regime $0<\hbar\omega<0.16\gamma_0$. The Fano factor increases rapidly in the regime $0.16\gamma_0<\hbar\omega<0.22\gamma_0$ to reach the magnitude $F\approx 0.1-0.12$. Then the Fano factor increases very slowly to reach the value $F\approx 0.13$ when the photon energy $\hbar\omega > 0.6\gamma_0$. The Fano factor of the unbalanced situation is much smaller than that of the balanced absorption situation. The resonant peaks of the Fano factor in the regime $0<\hbar\omega<0.16\gamma_0$ indicate the distinct different behaviors of shot noise and tunneling current versus photon energy. When the photon energy is small $\hbar\omega<0.21\gamma_0$, the Fano factors of type I $(7,7;-75,75)$ TCN and type III $(7,0;-75,150)$ TCN systems almost overlap each other, while there is an obvious difference as $\hbar\omega > 0.21\gamma_0$. The shot noise for the unbalanced absorption case also belongs to the sub-Poissonian case since $F<1$ when $eV=0.25\gamma_0$.

We present the shot noise and Fano factor for the unbalanced absorption cases in Figs. 7(a) and 7(b). It is clearly

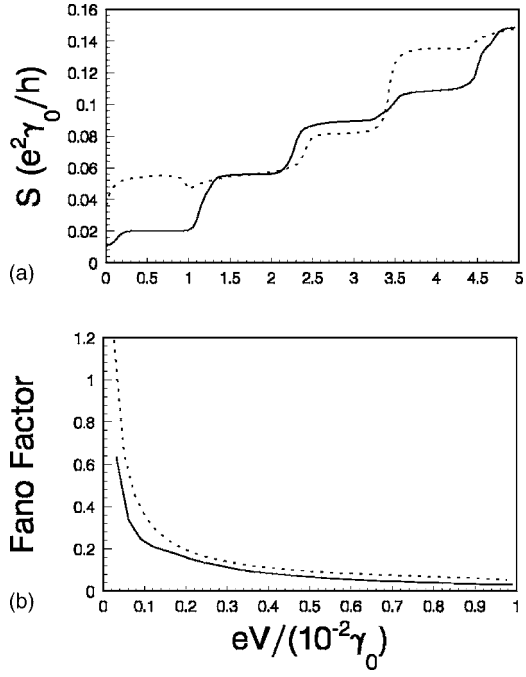

FIG. 7. Shot noise and Fano factor of unbalanced absorption cases versus source-drain bias. The parameters are chosen as $\phi=0$, $\hbar\omega=0.01\gamma_0$, and $\Gamma=0.001\gamma_0$. The solid and dotted curves are associated with $(7,7;-160,160)$, and $(7,7;-159,159)$ TCNs, respectively.

observed that the shot noise is nonzero for the two systems even though the corresponding current is zero for the symmetric system. This indicates that the shot noise induced by the pure photon absorption in the two leads contributes to the excess noise. Modified steps are obviously seen for the $(7,7,-159,159)$ TCN system. This modification comes from the unbalanced absorption procedure, and it cannot be observed in the balanced absorption situation compared with Fig. 2. The Fano factor drops rapidly as the source-drain bias increases, and it reaches the saturated value $F\sim 0.04$. As the source-drain bias is very small, $eV\sim 0$, the Fano factor is large enough to surpass 1, i.e., $F>1$ can be realized. This means that for our special case the super-Poissonian shot noise exists in the unbalanced absorption case although most of the shot noises belong to the sub-Poissonian cases.

IV. CONCLUDING REMARKS

We have investigated the shot noise of a system with a toroidal carbon nanotube coupled to two metal leads in the presence of microwave fields. The tunneling current operator is derived by determining the electron operators in different parts of the system, and the Landauer-Büttiker-like current operator is obtained from which we find the time-dependent current fluctuation correlations, and the spectral density of shot noise consequently. Our formula contains all effects concerning the TCN and applied microwave fields. The photon-assisted shot noise exhibits unusual behaviors due to the special properties of TCNs and the transport behaviors of electron in multichannel mesoscopic systems. The electron

transport is determined by the ac and dc driving forces, and the electrons tunnel in different channels of the TCN and sidebands. The quantum steps of shot noise with respect to the source-drain bias reflect the quantum nature of the TCN, as well as the applied microwave fields.

For the balanced absorption situation, the photon absorption and emission in the same lead are equal, and there exist no correlations between the sidebands of photon between different terminal currents. The shot noise disappears as the source-drain bias is removed at zero temperature. Nonlinear characteristics for the shot noise versus eV are displayed clearly for different TCN systems. The saturated value of the shot noise is suppressed by applying microwave fields, and the suppression is strongly associated with the structure of the TCN. The magnitude of the saturated Fano factor is around 0.4, and different TCN systems show different oscillation configurations. For the type II TCN system, the suppression can cause the Fano factor to reach 0.25 in a small regime of source-drain bias. This type of shot noise is sub-Poissonian.

For the unbalanced absorption situation, the absorption and emission of photons in the same terminal current are not necessarily equal, but the total absorption and emission of photons in the correlated currents are equal. The shot noise is contributed from the current correlations in the same lead as well as different leads. It is also contributed from the correlations of current branches tunneling in the same channel and different channels, which includes the correlations between different sidebands. There exists shot noise even if in the absence of source-drain bias. The photon energy plays the role of source-drain bias to induce shot noise, and shot noise may exist as the tunneling current becomes zero. In order to obtain obvious shot noise, we have to increase the photon energy to force the tunneling electron to overcome the threshold $\hbar\omega > \Delta$. The Fano factor of the unbalanced situation is much smaller than that of the balanced absorption situation for a definite value of $e\tilde{V}_{\gamma d}$ as the photon energy is small. Negative differential shot noise may be exhibited in the positive regime of eV, which shows rich physical behaviors of the shot noise. The shot noises of unbalanced system are sub-Poissonian as the source-drain bias eV increases to a definite value. However, super-Poissonian shot noise appears when the source-drain bias lies below this definite value. These resonant structures of shot noise indicate that the shot noise and tunneling current behave quite differently.

ACKNOWLEDGMENTS

This work was supported by a RGC grant from the SAR Government of Hong Kong under Grant No. HKU 7044/05P, and by the National Natural Science Foundation of China under the Grant No. 10375007.

*Mailing address.

[1] A. van der Ziel, *Noise in Solid State Devices and Circuits* (Wiley, New York, 1986).
[2] W. B. Davenport and W. L. Root, *An Introduction to the Theory of Random Signals and Noise* (IEEE Press, New York, 1987); *Noise in Devices and Circuits II*, edited by F. Danneville, F. Bonani, M. J. Deen, and M. E. Levinshtein (eds.), Proceedings of the SPIE Vol. 5470 (SPIE, Bellingham, Wa, 2004).
[3] H. B. Callen and T. W. Welton, Phys. Rev. **83**, 34 (1951).
[4] J. B. Johnson, Phys. Rev. **32**, 97 (1928); H. Nyquist, *ibid.* **32**, 110 (1928).
[5] M. Büttiker, Phys. Rev. Lett. **68**, 843 (1992); Phys. Rev. B **46**, 12485 (1992); Ya. M. Blanter and M. Büttiker, Phys. Rep. **336**, 1 (2000).
[6] M. J. M. de Jong and C. W. J. Beenakker, Phys. Rev. B **46**, 13400 (1992); **49**, 16070 (1994).
[7] H. K. Zhao, Phys. Lett. A **299**, 262 (2002); H. K. Zhao, Int. J. Mod. Phys. B **16**, 3503 (2002).
[8] W. Schottky, Ann. Phys. **57**, 541 (1918).
[9] Y. P. Li, D. C. Tsui, J. J. Heremans, J. A. Simmons, and G. W. Weimann, Appl. Phys. Lett. **57**, 774 (1990).
[10] M. Reznikov, M. Heiblum, H. Shtrikman, and D. Mahalu, Phys. Rev. Lett. **75**, 3340 (1995).
[11] A. Kumar, L. Saminadayar, D. C. Glattli, Y. Jin, and B. Etienne, Phys. Rev. Lett. **76**, 2778 (1996).
[12] V. V. Kuznetsov, E. E. Mendez, X. Zuo, G. L. Snider, and E. T. Croke, Phys. Rev. Lett. **85**, 397 (2000).
[13] A. N. Korotkov and K. K. Likharev, Phys. Rev. B **61**, 15975 (2000).
[14] O. M. Bulashenko and J. M. Rubí, Phys. Rev. B **64**, 045307 (2001); Phys. Rev. B **67**, 115322 (2003).
[15] G. Iannaccone, G. Lombardi, M. Macucci, and B. Pellegrini, Phys. Rev. Lett. **80**, 1054 (1998).
[16] S. S. Safonov, A. K. Savchenko, D. A. Bagrets, O. N. Jouravlev, Y. V. Nazarov, and E. Linfield, Phys. Rev. Lett. **91**, 136801 (2003).
[17] R. Martel, *et al.*, Appl. Phys. Lett. **73**, 2447 (1998).
[18] S. J. Tans, A. R. M. Verschueren, and C. Dekker, Nature (London) **393**, 49 (1998).
[19] Z. Yao, H. W. C. Postma, L. Balents, and C. Dekker, Nature (London) **402**, 273 (1999).
[20] J. W. Mintmire, B. I. Dunlap, and C. T. White, Phys. Rev. Lett. **68**, 631 (1992).
[21] S. J. Tans, M. H. Devoret, H. Dai, A. Thess, R. E. Smalley, L. J. Geerligs, and C. Dekker, Nature (London) **386**, 474 (1997).
[22] C. Zhou, J. Kong, and H. Dai, Phys. Rev. Lett. **84**, 5604 (2000).
[23] T. W. Odom, J. L. Huang, P. Kim, and C. M. Lieber, Nature (London) **391**, 62 (1998).
[24] A. Bachtold, C. Strunk, J. P. Salvetat, J. M. Bonard, L. Forró, T. Nussbaumer, and C. Schönenberger, Nature (London) **397**, 673 (1999).
[25] Y. Xue and S. Datta, Phys. Rev. Lett. **83**, 4844 (1999).
[26] H. Mehrez, J. Taylor, H. Guo, J. Wang, and C. Roland, Phys. Rev. Lett. **84**, 2682 (2000); C. Roland, M. Buongiorno Nardelli, J. Wang, and H. Guo, Phys. Rev. Lett. **84**, 2921 (2000).
[27] B. I. Dunlap, Phys. Rev. B **46**, 1933 (1992).
[28] S. Itoh, S. Ihara, and J. I. Kitakami, Phys. Rev. B **47**, 1703 (1993); S. Ihara, S. Itoh, and J. I. Kitakami, *ibid.* **47**, 12908

(1993).
[29] R. C. Haddon, Nature (London) **388**, 31 (1997).
[30] R. Martel, H. R. Shea, and Ph. Avouris, Nature (London) **398**, 299 (1999).
[31] M. F. Lin and D. S. Chuu, Phys. Rev. B **57**, 6731 (1998).
[32] H. K. Zhao, Phys. Lett. A **310**, 207 (2003); **308**, 226 (2003); **317**, 329 (2003).
[33] H. K. Zhao, Eur. Phys. J. B **33**, 365 (2003).
[34] H. K. Zhao and J. Wang, Phys. Lett. A **325**, 407 (2004).
[35] H. K. Zhao and J. Wang, Eur. Phys. J. B **40**, 93 (2004).
[36] H. K. Zhao and J. Wang, Phys. Rev. B **64**, 094505 (2001); H. K. Zhao, *ibid.* **63**, 205327 (2001).
[37] M. H. Pedersen and M. Büttiker, Phys. Rev. B **58**, 12993 (1998).
[38] V. S. Rychkov, M. L. Polianski, and M. Büttiker, Phys. Rev. B **72**, 155326 (2005).
[39] Q. F. Sun, J. Wang, and T. H. Lin, Phys. Rev. B **61**, 13032 (2000).
[40] A. P. Jauho, N. S. Wingreen, and Y. Meir, Phys. Rev. B **50**, 5528 (1994).
[41] R. Saito, G. Dresselhaus, and M. S. Dresselhaus, *Physical Properties of Carbon Nanotubes* (Imperial College Press, London, 1998).